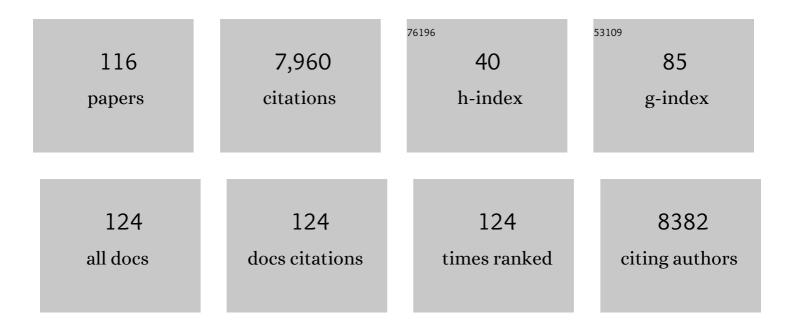
## **Robert F Dannals**

List of Publications by Year in descending order

Source: https://exaly.com/author-pdf/5021066/publications.pdf Version: 2024-02-01



#	Article	IF	CITATIONS
1	11C-Para-aminobenzoic acid PET imaging of S. aureus and MRSA infection in preclinical models and humans. JCI Insight, 2022, 7, .	2.3	11
2	Regional amyloid correlates of cognitive performance in ageing and mild cognitive impairment. Brain Communications, 2022, 4, fcac016.	1.5	5
3	PET/CT imaging of CSF1R in a mouse model of tuberculosis. European Journal of Nuclear Medicine and Molecular Imaging, 2022, 49, 4088-4096.	3.3	1
4	18F-labeled radiotracers for inÂvivo imaging of DREADD with positron emission tomography. European Journal of Medicinal Chemistry, 2021, 213, 113047.	2.6	7
5	First-in-human neuroimaging of soluble epoxide hydrolase using [18F]FNDP PET. European Journal of Nuclear Medicine and Molecular Imaging, 2021, 48, 3122-3128.	3.3	6
6	Imaging <i>Enterobacterales</i> infections in patients using pathogen-specific positron emission tomography. Science Translational Medicine, 2021, 13, .	5.8	49
7	Molecular imaging of the serotonin transporter availability and occupancy by antidepressant treatment in late-life depression. Neuropharmacology, 2021, 194, 108447.	2.0	10
8	Dynamic PET-facilitated modeling and high-dose rifampin regimens for <i>Staphylococcus aureus</i> orthopedic implant–associated infections. Science Translational Medicine, 2021, 13, eabl6851.	5.8	16
9	The Relationship of Varenicline Agonism of α4β2 Nicotinic Acetylcholine Receptors and Nicotine-Induced Dopamine Release in Nicotine-Dependent Humans. Nicotine and Tobacco Research, 2020, 22, 892-899.	1.4	8
10	High Availability of the α7-Nicotinic Acetylcholine Receptor in Brains of Individuals with Mild Cognitive Impairment: A Pilot Study Using <sup>18</sup> F-ASEM PET. Journal of Nuclear Medicine, 2020, 61, 423-426.	2.8	22
11	Osteopontin/secreted phosphoprotein-1 behaves as a molecular brake regulating the neuroinflammatory response to chronic viral infection. Journal of Neuroinflammation, 2020, 17, 273.	3.1	14
12	<sup>11</sup> C-PABA as a PET Radiotracer for Functional Renal Imaging: Preclinical and First-in-Human Study. Journal of Nuclear Medicine, 2020, 61, 1665-1671.	2.8	11
13	Dynamic imaging in patients with tuberculosis reveals heterogeneous drug exposures in pulmonary lesions. Nature Medicine, 2020, 26, 529-534.	15.2	87
14	PET imaging of soluble epoxide hydrolase in non-human primate brain with [18F]FNDP. EJNMMI Research, 2020, 10, 67.	1.1	10
15	Radiosynthesis and validation of [ <scp><i>Carboxy</i></scp> â€ <sup>11</sup> C]4â€ <scp>A</scp> minobenzoic acid ([ <sup>11</sup> <scp>C</scp> ] <scp>PABA</scp> ), a <scp>PET</scp> radiotracer for imaging bacterial infections. Journal of Labelled Compounds and Radiopharmaceuticals. 2019. 62. 28-33.	0.5	6
16	Radiosynthesis and validation of [5â€cyanoâ€ <i>N</i> à€(4â€{4â€{ <sup>11</sup> C]methylpiperazinâ€1â€yl)â€2â€(piperidinâ€1â€yl)phenyl) fu ([ <sup>11</sup> C]CPPC), a PET radiotracer for imaging CSF1R, a microgliaâ€specific marker. Journal of Labelled Compounds and Radiopharmaceuticals, 2019, 62, 903-908.	ranâ€2â€ 0.5	earþoxamide]
17	Effect of STN DBS on vesicular monoamine transporter 2 and glucose metabolism in Parkinson's disease. Parkinsonism and Related Disorders, 2019, 64, 235-241.	1.1	12
18	PET imaging of microglia by targeting macrophage colony-stimulating factor 1 receptor (CSF1R).	3.3	140

<sup>18</sup> Proceedings of the National Academy of Sciences of the United States of America, 2019, 116, 1686-1691.

#	Article	IF	CITATIONS
19	A side-by-side evaluation of [18F]FDOPA enantiomers for non-invasive detection of neuroendocrine tumors by positron emission tomography. Oncotarget, 2019, 10, 5731-5744.	0.8	3
20	Synthesis and Evaluation of a New 18F-Labeled Radiotracer for Studying the GABAB Receptor in the Mouse Brain. ACS Chemical Neuroscience, 2018, 9, 1453-1461.	1.7	7
21	<sup>18</sup> F-XTRA PET for Enhanced Imaging of the Extrathalamic α4β2 Nicotinic Acetylcholine Receptor. Journal of Nuclear Medicine, 2018, 59, 1603-1608.	2.8	15
22	An optimized radiosynthesis of [ <sup>18</sup> F]FNDP, a positron emission tomography radiotracer for imaging soluble epoxide hydrolase (sEH). Journal of Labelled Compounds and Radiopharmaceuticals, 2018, 61, 567-572.	0.5	8
23	Feasibility Evaluation of Myocardial Cannabinoid Type 1 Receptor ImagingÂinÂObesity. JACC: Cardiovascular Imaging, 2018, 11, 320-332.	2.3	24
24	Characterization of 3 Novel Tau Radiopharmaceuticals, <sup>11</sup> C-RO-963, <sup>11</sup> C-RO-643, and <sup>18</sup> F-RO-948, in Healthy Controls and in Alzheimer Subjects. Journal of Nuclear Medicine, 2018, 59, 1869-1876.	2.8	81
25	Preclinical Evaluation of <sup>18</sup> F-RO6958948, <sup>11</sup> C-RO6931643, and <sup>11</sup> C-RO6924963 as Novel PET Radiotracers for Imaging Tau Aggregates in Alzheimer Disease. Journal of Nuclear Medicine, 2018, 59, 675-681.	2.8	71
26	The distribution of the alpha7 nicotinic acetylcholine receptor in healthy aging: An in vivo positron emission tomography study with [18F]ASEM. NeuroImage, 2018, 165, 118-124.	2.1	27
27	Imaging glial activation in patients with post-treatment Lyme disease symptoms: a pilot study using [11C]DPA-713 PET. Journal of Neuroinflammation, 2018, 15, 346.	3.1	46
28	Noninvasive <sup>11</sup> C-rifampin positron emission tomography reveals drug biodistribution in tuberculous meningitis. Science Translational Medicine, 2018, 10, .	5.8	73
29	Peptide-Based <sup>68</sup> Ga-PET Radiotracer for Imaging PD-L1 Expression in Cancer. Molecular Pharmaceutics, 2018, 15, 3946-3952.	2.3	102
30	Imaging of Glial Cell Activation and White Matter Integrity in Brains of Active and Recently Retired National Football League Players. JAMA Neurology, 2017, 74, 67.	4.5	134
31	Development of a radioligand for imaging V 1a vasopressin receptors with PET. European Journal of Medicinal Chemistry, 2017, 139, 644-656.	2.6	8
32	Chemogenetics revealed: DREADD occupancy and activation via converted clozapine. Science, 2017, 357, 503-507.	6.0	813
33	Imaging α4β2 Nicotinic Acetylcholine Receptors (nAChRs) in Baboons with [18F]XTRA, a Radioligand with Improved Specific Binding in Extra-Thalamic Regions. Molecular Imaging and Biology, 2017, 19, 280-288.	1.3	11
34	Neuroimaging of translocator protein in patients with systemic lupus erythematosus: a pilot study using [ <sup>11</sup> C]DPA-713 positron emission tomography. Lupus, 2017, 26, 170-178.	0.8	25
35	PSMA-Based [18F]DCFPyL PET/CT Is Superior to Conventional Imaging for Lesion Detection in Patients with Metastatic Prostate Cancer. Molecular Imaging and Biology, 2016, 18, 411-419.	1.3	202
36	18F-FNDP for PET Imaging of Soluble Epoxide Hydrolase. Journal of Nuclear Medicine, 2016, 57, 1817-1822.	2.8	19

#	Article	IF	CITATIONS
37	An improved synthesis of the radiolabeled prostate-specific membrane antigen inhibitor, [ <sup>18</sup> F]DCFPyL. Journal of Labelled Compounds and Radiopharmaceuticals, 2016, 59, 439-450.	0.5	59
38	Development of a High-Affinity PET Radioligand for Imaging Cannabinoid Subtype 2 Receptor. Journal of Medicinal Chemistry, 2016, 59, 7840-7855.	2.9	47
39	Synthesis and quality control of [ <sup>18</sup> F]T807 for tau PET imaging. Journal of Labelled Compounds and Radiopharmaceuticals, 2016, 59, 411-415.	0.5	23
40	PET-measured longitudinal flow gradient correlates with invasive fractional flow reserve in CAD patients. European Heart Journal Cardiovascular Imaging, 2016, 18, jew116.	0.5	18
41	Comparison of Prostate-Specific Membrane Antigen–Based <sup>18</sup> F-DCFBC PET/CT to Conventional Imaging Modalities for Detection of Hormone-NaÃīve and Castration-Resistant Metastatic Prostate Cancer. Journal of Nuclear Medicine, 2016, 57, 46-53.	2.8	111
42	P4â€185: First inâ€human PET study of 3 novel tau radiopharmaceuticals: [ <sup>11</sup> C]RO6924963, [ <sup>11</sup> C]RO6931643, and [ <sup>18</sup> F]RO6958948. Alzheimer's and Dementia, 2015, 11, P850.	0.4	12
43	Bengt Långström-personal recollections of the gentle giant of short-lived radiotracers. Journal of Labelled Compounds and Radiopharmaceuticals, 2015, 58, 49-50.	0.5	0
44	Cannabinoid CB2 Receptors in a Mouse Model of Al² Amyloidosis: Immunohistochemical Analysis and Suitability as a PET Biomarker of Neuroinflammation. PLoS ONE, 2015, 10, e0129618.	1.1	83
45	Multiparametric Molecular Imaging Provides Mechanistic Insights into Sympathetic Innervation Impairment in the Viable Infarct Border Zone. Journal of Nuclear Medicine, 2015, 56, 457-463.	2.8	37
46	[ 125 I]Iodo-ASEM, a specific in vivo radioligand for α7-nAChR. Nuclear Medicine and Biology, 2015, 42, 488-493.	0.3	8
47	Mechanistic Insights into Sympathetic Neuronal Regeneration. Circulation: Cardiovascular Imaging, 2015, 8, e003507.	1.3	23
48	<sup>18</sup> F-DCFBC PET/CT for PSMA-Based Detection and Characterization of Primary Prostate Cancer. Journal of Nuclear Medicine, 2015, 56, 1003-1010.	2.8	180
49	Determination of [ <sup>11</sup> C]Rifampin Pharmacokinetics within Mycobacterium tuberculosis-Infected Mice by Using Dynamic Positron Emission Tomography Bioimaging. Antimicrobial Agents and Chemotherapy, 2015, 59, 5768-5774.	1.4	47
50	Brown Adipose Tissue Response Dynamics: In Vivo Insights with the Voltage Sensor 18F-Fluorobenzyl Triphenyl Phosphonium. PLoS ONE, 2015, 10, e0129627.	1.1	12
51	Doseâ€dependent, saturable occupancy of the metabotropic glutamate subtype 5 receptor by fenobam as measured with [ <sup>11</sup> C]ABP688 PET imaging. Synapse, 2014, 68, 565-573.	0.6	21
52	Positron emission tomography radioligands for the opioid system. Journal of Labelled Compounds and Radiopharmaceuticals, 2013, 56, 187-195.	0.5	18
53	Characterization of [11C]RO5013853, a novel PET tracer for the glycine transporter type 1 (GlyT1) in humans. NeuroImage, 2013, 75, 282-290.	2.1	26
54	Pre-clinical characterization of [11C]R05013853 as a novel radiotracer for imaging of the glycine transporter type 1 by positron emission tomography. NeuroImage, 2013, 75, 291-300.	2.1	16

#	Article	IF	CITATIONS
55	Dissociative Changes in the B <sub>max</sub> and K <sub>D</sub> of Dopamine D <sub>2</sub> /D <sub>3</sub> Receptors with Aging Observed in Functional Subdivisions of the Striatum: A Revisit with an Improved Data Analysis Method. Journal of Nuclear Medicine, 2012, 53, 805-812.	2.8	17
56	Radiosynthesis of [5â€{ <sup>11</sup> C]methanesulfonylâ€2â€{( <i>S</i> )â€2,2,2â€trifluoroâ€1â€methylâ€ethoxy)â€phenyl] ([ <sup>11</sup> C]RO5013853), a novel PET tracer for the glycine transporter type I (GlyT1). Journal of Labelled Compounds and Radiopharmaceuticals, 2011, 54, 702-707.	â€{5â€{tetr	ahygroâ€pyra
57	Radiosynthesis of the α4β2 nicotinic acetylcholine receptor ligand: 5-((1-[11C]-methyl-2-(S)-pyrrolidinyl)methoxy)-2-chloro-3-((E)-2-(2-fluoropyridin-4-yl)vinyl)pyridine. Journal of Labelled Compounds and Radiopharmaceuticals, 2006, 49, 459-462.	0.5	0
58	Synthesis of a mGluR5 antagonist using [11C]copper(I) cyanide. Journal of Labelled Compounds and Radiopharmaceuticals, 2006, 49, 829-834.	0.5	22
59	Synthesis of [11C]gefitinib for imaging epidermal growth factor receptor tyrosine kinase with positron emission tomography. Journal of Labelled Compounds and Radiopharmaceuticals, 2006, 49, 883,888 Synthesis of	0.5	19
60	1-(2,4-dichlorophenyl)-4-cyano-5-(4-[11C]methoxyphenyl)-N-(piperidin-1-yl)-1H-pyrazole-3-carboxamide ([11C]JHU75528) and 1-(2-bromophenyl)-4-cyano-5-(4-[11C]methoxyphenyl)-N-(piperidin-1-yl)-1H-pyrazole-3-carboxamide ([11C]JHU75575) as potential radioligands for PET imaging of cerebral cannabinoid receptor. Journal of	0.5	32
61	Labelled Compounds and Radiopharmaceuticals, 2006, 49, 1021-1036. Characterization of dose dependent norepinephrine transporter blockade by atomoxetine in human brain using 11C MeNER PET. Journal of Cerebral Blood Flow and Metabolism, 2005, 25, S599-S599.	2.4	2
62	Radiosynthesis of 3-[18F]fluoropropyl and 4-[18F]fluorobenzyl triarylphosphonium ions. Journal of Labelled Compounds and Radiopharmaceuticals, 2004, 47, 469-476.	0.5	52
63	Neural basis of alertness and cognitive performance impairments during sleepiness II. Effects of 48 and 72 h of sleep deprivation on waking human regional brain activity. Thalamus & Related Systems, 2003, 2, 199.	0.5	91
64	<sup>11</sup> C-MCG: Synthesis, Uptake Selectivity, and Primate PET of a Probe for Glutamate Carboxypeptidase II (NAALADase). Molecular Imaging, 2002, 1, 153535002002021.	0.7	27
65	[11C]-GR89696, a potent kappa opiate receptor radioligand; in vivo binding of the R and S enantiomers. Nuclear Medicine and Biology, 2002, 29, 47-53.	0.3	34
66	Radiosynthesis of [11C]paclitaxel. Journal of Labelled Compounds and Radiopharmaceuticals, 2002, 45, 471-477.	0.5	17
67	Use of Positron Emission Tomography to Study AT1 Receptor Regulation In Vivo. Journal of the American Society of Nephrology: JASN, 2001, 12, 1350-1358.	3.0	37
68	Synthesis and initialin vitro characterization of 6-[18F]fluoro-3-(2(S)-azetidinylmethoxy)pyridine, a high-affinity radioligand for central nicotinic acetylcholine receptors. Journal of Labelled Compounds and Radiopharmaceuticals, 2000, 43, 413-423.	0.5	16
69	Neural basis of alertness and cognitive performance impairments during sleepiness. I. Effects of 24 h of sleep deprivation on waking human regional brain activity. Journal of Sleep Research, 2000, 9, 335-352.	1.7	914
70	Column-switching HPLC for the analysis of plasma in PET imaging studies. Nuclear Medicine and Biology, 2000, 27, 627-630.	0.3	191
71	Effect of tracer metabolism on PET measurement of [11C]pyrilamine binding to histamine H1 receptors. Annals of Nuclear Medicine, 1999, 13, 101-107.	1.2	9
	Doses of GBR12909 that suppress cocaine self-administration in non-human primates substantially		

Doses of GBR12909 that suppress cocaine self-administration in non-human primates substantially occupy dopamine transporters as measured by [11C] WIN35,428 PET scans. , 1999, 32, 44-50.

50

#	Article	IF	CITATIONS
73	GBR12909 attenuates amphetamine-induced striatal dopamine release as measured by [11C]raclopride continuous infusion PET scans. Synapse, 1999, 33, 268-273.	0.6	50
74	Synthesis of N1â€2-([18F]fluoroethyl)naltrindole ([18F]FEtNTI): a radioligand for positron emission tomographic studies of delta opioid receptors. Journal of Labelled Compounds and Radiopharmaceuticals, 1999, 42, 43-54.	0.5	11
75	Synthesis of [18F] SR144385: a selective radioligand for positron emission tomographic studies of brain cannabinoid receptors. Journal of Labelled Compounds and Radiopharmaceuticals, 1999, 42, 589-596.	0.5	16
76	[11C]-methyl 4-[(3,4-dichlorophenyl)acetyl]-3-[(1-pyrrolidinyl)methyl]-1-piperazinecarboxylate ([11C]GR89696): synthesis and in vivo binding to kappa opiate receptors. Nuclear Medicine and Biology, 1999, 26, 737-741.	0.3	28
77	In vivo detection of short- and long-term MDMA neurotoxicity?a positron emission tomography study in the living baboon brain. Synapse, 1998, 29, 183-192.	0.6	141
78	Nicotine induced up-regulation of nicotinic receptors in CD-1 mice demonstrated with an in vivo radiotracer: Gender differences. Synapse, 1998, 30, 116-118.	0.6	40
79	Cerebral Glucose Utilization Is Reduced in Second Test Session. Journal of Cerebral Blood Flow and Metabolism, 1997, 17, 704-712.	2.4	43
80	Imaging of ?- and ?-opioid receptors in temporal lobe epilepsy by positron emission tomography. Annals of Neurology, 1997, 41, 358-367.	2.8	107
81	Synthesis of a radioiodinated analog of epibatidine: (A±)-exo-2-(2-iodo-5-pyridyl)-7-azabicyclo[2.2.1]heptane for in vitro and in vivo studies of nicotinic acetylcholine receptors. Journal of Labelled Compounds and Radiopharmaceuticals, 1997, 39, 39-48.	0.5	21
82	Synthesis of 3-[(1-[11C]methyl-2(S)-pyrrolidinyl) methoxy]pyridine and 3-[(1-[11C]methyl-2(R)-pyrrolidinyl) methoxy]pyridine: Radioligands for in vivo studies of neuronal nicotinic acetylcholine receptors. Journal of Labelled Compounds and Radiopharmaceuticals, 1997, 39, 425-431.	0.5	10
83	[125/123I]IPH: A radioiodinated analog of epibatidine for in vivo studies of nicotinic acetylcholine receptors. , 1997, 26, 392-399.		52
84	External monitoring of cerebral nicotinic acetylcholine receptors in living mice. Synapse, 1997, 27, 378-380.	0.6	4
85	Synthesis of 3-[(1-[11C]methyl-2(S)-pyrrolidinyl) methoxy]pyridine and 3-[(1-[11C]methyl-2(R)-pyrrolidinyl) methoxy]pyridine: Radioligands for in vivo studies of neuronal nicotinic acetylcholine receptors. Journal of Labelled Compounds and Radiopharmaceuticals, 1997, 39, 425-431.	0.5	2
86	Assessing neuroreceptor occupancy by continuous infusion of carbon-11 labeled radioligands. European Journal of Nuclear Medicine and Molecular Imaging, 1996, 23, 141-144.	2.2	2
87	Synthesis of a radiotracer for studying nicotinic acetylcholine receptors: (+/â^)·exo-2-(2-[18F]fluoro-5-pyridyl)-7-azabicyclo[2.2.1]heptane. Journal of Labelled Compounds and Radiopharmaceuticals, 1996, 38, 355-365.	0.5	67
88	Imaging of ? opioid receptors in human brain by N1?- ([11C]methyl)naltrindole and PET. , 1996, 24, 19-28.		69
89	Increased mu opioid receptor binding detected by PET in cocaine–dependent men is associated with cocaine craving. Nature Medicine, 1996, 2, 1225-1229.	15.2	250
90	Synthesis of N1′-([11C]methyl)naltrindole ([11C]MeNTI): A radioligand for positron emission tomographic studies of delta opioid receptors. Journal of Labelled Compounds and Radiopharmaceuticals, 1995, 36, 137-145.	0.5	21

#	Article	IF	CITATIONS
91	Synthesis of carbon-11 labeled methylcarbamates from [11C]-methylchloroformate. Journal of Labelled Compounds and Radiopharmaceuticals, 1995, 36, 365-371.	0.5	8
92	Development of imaging agents for the dopamine transporter. Medicinal Research Reviews, 1995, 15, 419-444.	5.0	33
93	Positron emission tomography imaging of serotonin transporters in the human brain using [11C](+)McN5652. Synapse, 1995, 20, 37-43.	0.6	161
94	Cerebral Glucose Utilization in Polysubstance Abuse. Neuropsychopharmacology, 1995, 13, 21-31.	2.8	48
95	Cerebral Glucose Utilization in Polysubstance Abuse. Neuropsychopharmacology, 1995, 13, 21-31.	2.8	10
96	Buprenorphine Reduces Cerebral Glucose Metabolism in Polydrug Abusers. Neuropsychopharmacology, 1994, 10, 157-170.	2.8	25
97	Decreased hippocampal muscarinic cholinergic receptor binding measured by1231-iododexetimide and single-photon emission computed tomography in epilepsy. Annals of Neurology, 1993, 34, 235-238.	2.8	35
98	Positron emission tomographic imaging of the dopamine transporter with11C-WIN 35,428 reveals marked declines in mild Parkinson's disease. Annals of Neurology, 1993, 34, 423-431.	2.8	321
99	Noncompartmental and compartmental modeling of the kinetics of carbon-11 labeled pyrilamine in the human brain. Synapse, 1993, 15, 263-275.	0.6	17
100	In vivo imaging of dopamine reuptake sites in the primate brain using single photon emission computed tomography (SPECT) and iodine-123 labeled RTI-55. Synapse, 1992, 10, 169-172.	0.6	85
101	[123/125I]RTI-55, an in vivo label for the serotonin transporter. Synapse, 1992, 11, 134-139.	0.6	70
102	In vivo studies of [1251]iodobenzamide and [11C]iodobenzamide: A ligand suitable for positron emission tomography imaging of cerebral D2 dopamine receptors. Synapse, 1992, 12, 236-241.	0.6	6
103	Effects of Vasopressin on Blood-Brain Transfer of Methionine in Dogs. Journal of Neurochemistry, 1992, 59, 1421-1429.	2.1	11
104	Imaging Muscarinic Cholinergic Receptors in Human Brain in vivo with SPECT, [123I]4-lododexetimide, and [123I]4-lodolevetimide. Journal of Cerebral Blood Flow and Metabolism, 1992, 12, 562-570.	2.4	60
105	Synthesis of a Radiotracer for Studying k-Subtype Opiate Receptors: N-[11C-methyl]-N-(trans-2-pyrrolidinyl-cyclohexyl)-3,4-dichlorophenylacetamide ([11C](±)U-50488H). Journal of Labelled Compounds and Radiopharmaceuticals, 1992, 31, 81-89.	0.5	12
106	Quantification of Human Opiate Receptor Concentration and Affinity Using High and Low Specific Activity [ <sup>11</sup> C]Diprenorphine and Positron Emission Tomography. Journal of Cerebral Blood Flow and Metabolism, 1991, 11, 204-219.	2.4	94
107	Quantification of mu and non-mu opiate receptors in temporal lobe epilepsy using positron emission tomography. Annals of Neurology, 1991, 30, 3-11.	2.8	189
108	Mania after brain injury: Neuroradiological and metabolic findings. Annals of Neurology, 1990, 27, 652-659.	2.8	238

#	Article	IF	CITATIONS
109	Selective hypometabolism in the inferior frontal lobe in depressed patients with Parkinson's disease. Annals of Neurology, 1990, 28, 57-64.	2.8	400
110	Facile synthesis of [11C]buprenorphine for positron emission tomographic studies of opioid receptors. International Journal of Radiation Applications and Instrumentation Part A, Applied Radiation and Isotopes, 1990, 41, 745-752.	0.5	19
111	Mu-opiate receptors measured by positron emission tomography are increased in temporal lobe epilepsy. Annals of Neurology, 1988, 23, 231-237.	2.8	253
112	Localization of serotonin 5-HT2 receptors in living human brain by positron emission tomography using N1-([11C]-methyl)-2-BR-LSD. Synapse, 1987, 1, 393-398.	0.6	94
113	Synthesis of carbon-11 labeled diprenorphine: A radioligand for positron emission tomographic studies of opiate receptors. Tetrahedron Letters, 1987, 28, 4015-4018.	0.7	38
114	Imaging Opiate Receptors in the Human Brain by Positron Tomography. Journal of Computer Assisted Tomography, 1985, 9, 231-236.	0.5	237
115	Radiosynthesis of an opiate receptor binding radiotracer: [11C]carfentanil. The International Journal of Applied Radiation and Isotopes, 1985, 36, 303-306.	0.7	136
116	In vivo studies of opiate receptors. Annals of Neurology, 1984, 15, 85-92.	2.8	37